

**Charge oscillation in multiphoton and tunneling ionization of rare-gas dimers**Min Li,<sup>1</sup> Hong Liu,<sup>1</sup> Cong Wu,<sup>1</sup> Yongkai Deng,<sup>1</sup> Chengyin Wu,<sup>1,2</sup> Qihuang Gong,<sup>1,2</sup> and Yunquan Liu<sup>1,2,\*</sup><sup>1</sup>*Department of Physics and State Key Laboratory for Mesoscopic Physics, Peking University, Beijing 100871, China*<sup>2</sup>*Collaborative Innovation Center of Quantum Matter, Beijing 100871, China*

(Received 3 January 2013; revised manuscript received 18 March 2013; published 14 February 2014)

We perform a comparison study on strong-field ionization of the rare-gas dimers ( $\text{Kr}_2$  and  $\text{Ar}_2$ ) with their rare-gas monomers (Kr and Ar) in infrared laser fields at wavelengths of 795 and 1320 nm in the intensity range of  $(0.4\text{--}2)\times 10^{14}$  W/cm<sup>2</sup>. The photoelectron longitudinal momentum distributions of the rare-gas dimers reveal prominent intensity and wavelength dependence. Compared to that of the rare-gas monomers, photoelectrons obtain smaller drift momentum for multiphoton ionization of the dimers at the same laser intensity. However, in the tunneling regime, the ionization of the dimers shows similar photoelectron longitudinal momentum distributions with the monomers at the same laser intensity. We identify that, for multiphoton ionization of the dimers, the recaptured electrons during rescattering prefer to start charge oscillation in the dimer ions, which is coupled by the laser field. When the laser field decreases, the charge oscillated electrons will be released and will have less chance to obtain larger drift momentum from the laser field. The ionization of the dimers in the tunneling regime behaves much like the ionization of one of the two constituent, nearly unperturbed rare-gas atoms.

DOI: [10.1103/PhysRevA.89.025402](https://doi.org/10.1103/PhysRevA.89.025402)

PACS number(s): 32.80.Rm, 32.80.Wr, 42.50.Hz

Rare-gas (RG) dimers have attracted considerable research interest as prototype van der Waals homonuclear molecules. Because of the extraordinarily large internuclear distances ranging from 2.97 Å for  $\text{He}_2$  to 4.36 Å for  $\text{Xe}_2$  and small binding energies (e.g., 12 meV for  $\text{Ar}_2$ ), they often are treated as if each atom is nearly independent, which is very different from those normal hard bonding molecules. Photoionization of the RG dimers in an intense laser pulse is expected to proceed with electron delocalization. One of the reasons for the great interest in photoionization of the RG dimers by x-ray radiation was that the relaxation via electron emission can arise from energy or electron exchange between neighboring sites and result in so-called interatomic Coulombic decay [1,2]. On the other hand, there is also increasing interest in photoionization of dimers with intense infrared laser pulses, e.g., two-center interference [3] and double or multiple ionization [4–6]. Photoionization of molecules by intense infrared laser pulses is very different from the interaction using x-ray lasers because the electrons in the outermost orbitals are usually involved. The study on the ionization of the RG dimers by the infrared laser fields is highly important for the understanding of strong-field molecular ionization with much larger internuclear distance.

We study the photoelectron momentum spectra of strong-field ionization of the RG dimers ( $\text{Ar}_2$  and  $\text{Kr}_2$ ), as well as their RG monomers (Ar and Kr), at wavelengths of 795 and 1320 nm in the intensity range of  $(0.4\text{--}2)\times 10^{14}$  W/cm<sup>2</sup>. Using linearly polarized laser pulses, we observe that the photoelectron longitudinal momentum distributions (along the laser polarization axis) of the RG dimers are much narrower than that of the monomers at the same laser intensity in the multiphoton regime ( $\gamma > 1$ ). Here,  $\gamma$  is the Keldysh parameter [7] given by  $\gamma = \sqrt{I_p/2U_p}$  [ $I_p$ : ionization potential;  $U_p = E_0^2/4\omega^2$ : ponderomotive potential with  $E_0$  the laser field amplitude and  $\omega$  its frequency; atomic units (a.u.) are used throughout unless specified]. Instead, in the tunneling regime ( $\gamma < 1$ ), the photoelectron longitudinal momentum distributions of the

dimers and the monomers show similar shape at the same laser intensity. We identify that, for multiphoton ionization of the dimers, the recaptured electrons during rescattering will prefer to oscillate in the potential of the dimer ions mediated by the laser field after their revisiting. The charge oscillated electrons will miss the maximum of field strength and will be released. The electrons will have less chance to obtain drift momentum from the laser field. In contrast, tunneling ionization of the dimers is a practical ionization of one of the two constituent, nearly unperturbed RG atoms. Recollision probability will decrease because the tunneled electron will experience a long excursion, and the probability of charge oscillation in the dimer ions is substantially suppressed in the tunneling regime.

Experimentally, we used Ti:sapphire laser pulses with a width of 25 fs at a repetition rate of 3 kHz centered at a wavelength of 795 nm. We measured fully differential photoelectron momentum distributions with cold target recoil ion momentum spectroscopy (COLTRIMS) [8,9] (for the principle see [10]) with the photoelectron momentum resolution  $\sim 0.02$  a.u. along the time-of-flight direction and  $\sim 0.05$  a.u. along the transverse direction. The  $\text{Ar}_2$  and  $\text{Kr}_2$  dimers were naturally produced by the supersonic expansion of Ar and Kr gases into high vacuum chamber (better than  $5 \times 10^{-10}$  mbar) with a nozzle of 30  $\mu\text{m}$  using a driving pressure of 2 bars. Weak electric ( $\sim 3$  V/cm) and magnetic ( $\sim 5$  G) fields were applied along the time-of-flight axis. Ions and photoelectrons were measured with two position-sensitive channel plate detectors, respectively. From the time-of-flight and position on the detectors, the full momentum vectors of particles were constructed. We measured the photoelectrons in coincidence with their singly charged parent atomic (or dimer) ions. To avoid false coincidence signal, we kept the electron rate below 0.3 per laser pulse. The laser polarization direction was along the time-of-flight axis. The laser intensity was controlled with a pair of thin-film polarizers.

Before presenting the experimental results of the RG dimers, it is highly necessary to study the effect of the ionization potential on the photoelectron momentum

\*Yunquan.liu@pku.edu.cn

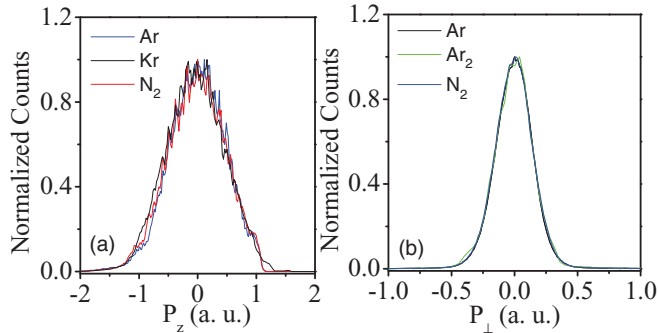


FIG. 1. (Color online) (a) The photoelectron longitudinal momentum distributions of single ionization of Ar, Kr, and  $N_2$  in linearly polarized laser fields at the intensity of  $1.2 \times 10^{14}$  W/cm<sup>2</sup> at 795 nm ( $\gamma \sim 1.04$  for Ar). (b) The transverse momentum distributions of single ionization of Ar,  $Ar_2$ , and  $N_2$  in a circularly polarized laser field at the intensity of  $2.5 \times 10^{14}$  W/cm<sup>2</sup> at 795 nm ( $\gamma \sim 1.02$  for Ar).

distributions because the RG dimers have ionization potentials close (i.e., an energy difference less than 2 eV) to those of the monomers. We first measured the photoelectron longitudinal momentum distributions of single ionization of Ar ( $I_p = 15.76$  eV) and  $N_2$  ( $I_p = 15.58$  eV) using the mixture gas Ar/ $N_2$  at the same laser intensity of  $1.2 \times 10^{14}$  W/cm<sup>2</sup> ( $\gamma \sim 1.04$  for Ar). As shown in Fig. 1(a), the overall photoelectron momentum distributions show a very similar shape in linearly polarized laser pulses (795 nm, 25 fs) at the same laser intensity for those targets with close ionization potentials. Whether increasing or decreasing the laser intensity, the overall shape of photoelectron longitudinal momentum distributions of Ar and  $N_2$  at the same laser condition does not change too much [10]. Those results can be well understood within the scenario of strong-field approximation (SFA) [11,12]. The longitudinal momentum distribution is expected to reveal the same shape since the photoelectron longitudinal momentum is only determined by the laser field. The slight difference of ionization potential has less evident effect on the overall momentum distribution. For instance, for Kr atoms with a lower ionization potential of  $\sim 14.0$  eV, the overall momentum distribution [black curve in Fig. 1(a)] also shows similar shape at the same laser intensity, as compared with that of Ar and  $N_2$ .

The ionization potential of  $Ar_2$  is  $\sim 14.52$  eV [13], which is in between that of Kr and Ar. With the above discussion in mind, it seems reasonable to expect that the overall photoelectron longitudinal momentum distributions of  $Ar_2$  would reveal distribution similar to Ar. However, as seen in Fig. 2(a) for the measured momentum distributions of single ionization of  $Ar_2/Ar$  at 795 nm in the intensity range of  $(0.4\text{--}2) \times 10^{14}$  W/cm<sup>2</sup>, the photoelectron longitudinal momentum distribution of the dimers is much narrower than that of the monomers at the same laser intensity. Decreasing the laser intensity, the difference is more evident. The narrower longitudinal momentum distributions imply that the photoelectrons emitted from multiphoton ionization of the dimers do not obtain drift momentum as large as that of the monomers from the laser field at the same intensity. The phenomenon is also observed for the targets of Kr/ $Kr_2$  ( $Kr_2$ :  $I_p = 12.87$  eV [14]) in multiphoton ionization, as seen in Fig. 2(b).

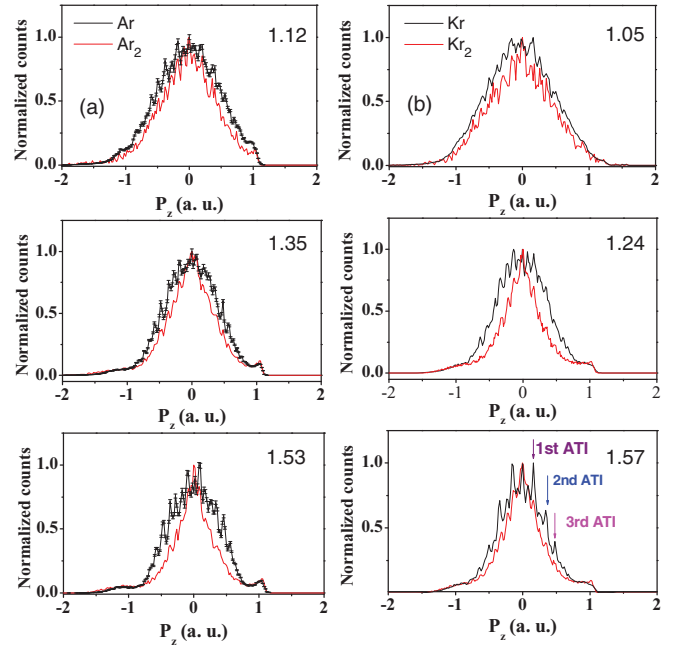


FIG. 2. (Color online) The photoelectron longitudinal momentum distributions of  $Ar_2/Ar$  (left column) and  $Kr_2/Kr$  (right column) in linearly polarized laser fields at the intensity range of  $(0.4\text{--}2) \times 10^{14}$  W/cm<sup>2</sup> at 795 nm. Above-threshold ionization peaks are clearly observed in longitudinal momentum spectra for RG atoms (e.g., see the right bottom figure). The Keldysh parameters for Ar and Kr atoms are labeled at the right top corner in each panel.

For the atoms with much higher ionization potentials, i.e., Ne and He, the longitudinal momentum distributions are much narrower than those of RG atoms with lower ionization potentials at the same laser intensity because of strong Coulomb attraction on photoelectrons after the tunneling [15]. The narrower momentum distributions of the dimer ions may simply imply that the “appearance ionization potential” of the dimers is much larger than that of the monomers in the multiphoton regime.

To test this hypothesis, we further measured the ionization rate of the dimers and the monomers with respect to the laser intensity. We found that the ratio of  $RG_2^+/RG^+$  increases slightly with decreasing the laser intensity. For example, for a 795-nm laser pulse, the rate ratio of  $Ar_2^+/Ar^+$  is about 0.15 at the intensity of  $0.4 \times 10^{14}$  W/cm<sup>2</sup> and it is about 0.08 at the intensity of  $2 \times 10^{14}$  W/cm<sup>2</sup>. Since the concentration of the dimers in the supersonic gas is  $\sim 10\%$  of atoms, the ionization rate of the dimers is really comparable with that of the monomers at the same intensity. Thus, the narrow momentum distribution does not result from the “larger appearance ionization potential” because the ionization rate will exponentially decrease with increasing the ionization potential according to the tunneling theory [16].

At 795 nm, increasing the laser intensity to the tunneling regime, the difference of momentum distributions between the dimers and the monomers becomes less evident. To investigate tunneling ionization of the dimers, we further produced linearly polarized 1320-nm radiation generated by an optical parametric amplification (OPA) system. The estimated

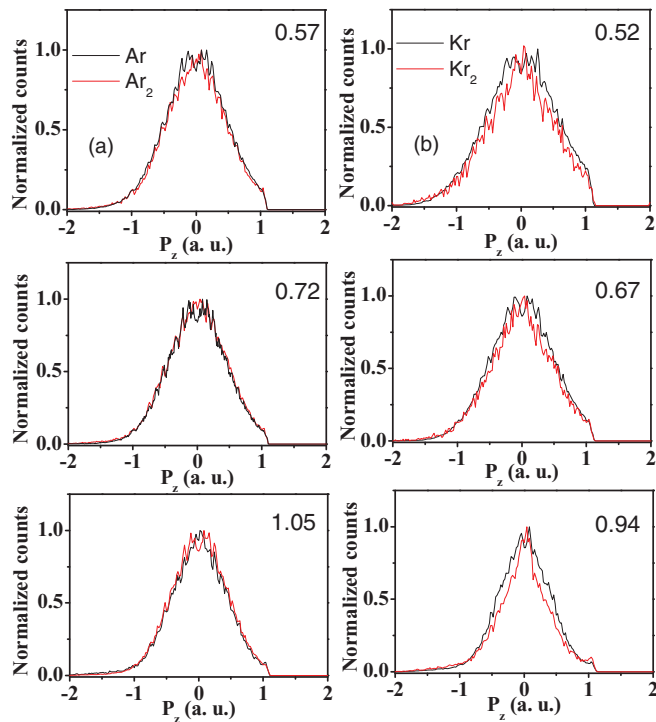


FIG. 3. (Color online) The photoelectron longitudinal momentum distributions of  $\text{Ar}_2/\text{Ar}$  (left column) and  $\text{Kr}_2/\text{Kr}$  (right column) in linearly polarized laser fields at the intensity range of  $(0.4\text{--}2) \times 10^{14} \text{ W/cm}^2$  at 1320 nm. The Keldysh parameters for Ar and Kr atoms are labeled at the right top corner in each panel.

pulse duration was about 30–35 fs. Using linearly polarized 1320-nm radiation, we have also measured the photoelectron longitudinal momentum distributions of  $\text{Ar}/\text{Ar}_2$  and  $\text{Kr}/\text{Kr}_2$  at the same laser intensity, as shown in Figs. 3(a) and 3(b), respectively. One can observe that photoelectrons of the dimers in the tunneling regime achieve similar longitudinal momenta as compared with those of the monomers.

In order to look into pure tunneling effect, we also measured the transverse momentum for Ar,  $\text{N}_2$ , and  $\text{Ar}_2$  in circularly polarized laser fields using the mixture gas of  $\text{N}_2/\text{Ar}$  at 795 nm at the intensity of  $2.5 \times 10^{14} \text{ W/cm}^2$  ( $\gamma \sim 1.02$  for Ar). We have two purposes for using circularly polarized laser fields: (i) The effect of electron recollision [17] is substantially suppressed; (ii) the momentum distribution perpendicular to the polarization plane can directly reflect the ionization potential and the laser field. According to the tunneling model [16], the momentum transverse to the laser field is predicted with a distribution of  $\exp(-p_\perp^2/\sigma^2)$  (the width is given by  $\sigma_\perp = [|\overline{E(t)}|/\sqrt{2I_P}]^{1/2}$ ). As shown in Fig. 1(b), in circularly polarized fields, the difference of the transverse momentum distributions of Ar,  $\text{N}_2$ , and  $\text{Ar}_2$  is less evident although the electronic structure of those targets is dramatically different.

Obviously, electron recollision plays a decisive role in strong-field ionization of the dimers in linearly polarized light fields. As is known, one of the natural consequences of electron recollision in linearly polarized fields is frustrated ionization [18,19], in which a fraction of tunneled electrons

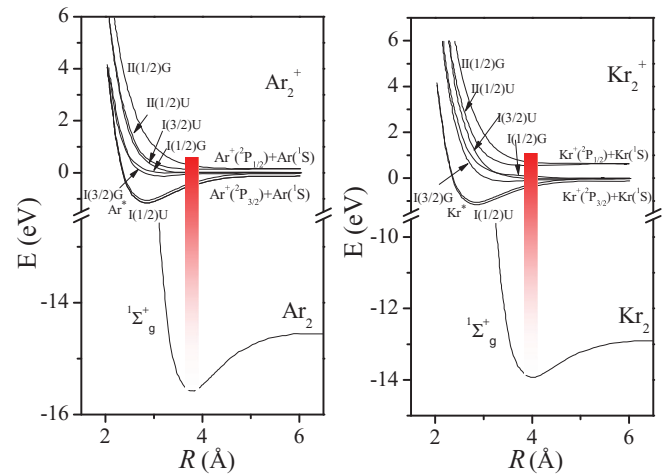


FIG. 4. (Color online) The potential curves of the lowest states for Ar and Kr dimers and their dimer ions. The shaded area represents the Franck-Condon region of the neutral ground states.

can be recaptured by the ionic potential mediated by the laser field [20]. The recaptured probability will decrease with increasing the laser intensity and the wavelength because the returned electrons will obtain a larger momentum from the laser field and experience a long excursion before recollision.

For strong-field ionization of atoms, the recaptured electrons are mostly stabilized in Rydberg states. However, for strong-field ionization of the RG dimers with larger internuclear distance, the recaptured electrons can move easily in the potential of the dimer ions coupled by the linearly polarized laser field. In order to understand ionization dynamics of the dimers, we illustrate the potential energy curves of the lowest states of  $\text{Ar}_2^+/\text{Ar}_2$  and  $\text{Kr}_2^+/\text{Kr}_2$  in Figs. 4(a) and 4(b), respectively. The potential curves are taken from [21]. Because the equilibrium internuclear distances of the dimer ions are much less than those of the neutral dimers, the Franck-Condon region is unfavorable for the transitions to the lowest vibrational levels of the ground state of the dimer ions. Since the motion of electrons occurs in a time scale much shorter than the nuclear motion (vibration and rotation), electron dynamics is more relevant in ultrashort laser pulse. In the Franck-Condon region, the energy splitting for the allowed transition among the ionic states is in a range of 0.5–1 eV at such a large internuclear distance. Therefore, when the recolliding electrons are captured by the dimer ions, charge spreading will happen, starting the oscillation among the ionic states. The situation is much like charge resonance enhanced ionization (CREI) of  $\text{H}_2^+$  at a larger internuclear distance of  $\sim 7\text{--}10$  a.u. [22]. Differently, it does not need much time to reach such larger internuclear distance for the dimer ions.

When the dynamic evolution of an excited electron is induced in the dimer ions, the outcome will certainly have an influence on the final photoelectron momentum distribution. The estimated period of the charge oscillation is about 4–8 fs, which is much longer than the period of the laser pulse (2.7 fs for 800 nm). The electrons will be trapped in the charge oscillation states of the dimer ions and do not follow the laser field. Therefore, photoelectrons of multiphoton ionization of dimers have less chance to obtain drift momentum from the laser field. For a

long-wavelength pulse, the charge oscillation period is close to the laser period (4.4 fs for a 1320-nm laser). The electrons can follow the laser field and will finally acquire larger longitudinal drift momentum from the laser field. In this case, tunneling ionization of the dimers behaves much like the ionization of one of the atomic constituent, nearly unperturbed RG atoms.

In the multiphoton regime, electron recapture will facilitate the charge oscillation in the dimer ions. Increasing the laser intensity, i.e., in the tunneling regime, the recapture probability decreases because the recolliding electrons pick up much energy from the laser field. The recolliding electrons have less chance to be recaptured, and will not facilitate the charge oscillation in the dimer ions. The electrons can follow the laser field to achieve much drift momentum. Using a long-wavelength laser pulse, the probability of electron recapture into the dimer ions also decreases because the tunneled electrons have a long excursion before recollision. Thus, tunneling ionization of the RG dimers behaves similarly as the RG atoms because the charge oscillation probability is suppressed. Increasing the laser ellipticity, such discrepancy also becomes less because the recapture probability decreases.

The narrower longitudinal momentum distributions observed in multiphoton ionization of the dimers can be basically understood within the picture of the charge oscillation facilitated by the recapture of recolliding electrons in linearly polarized fields. This will give rise to three important outcomes. First, when the field strength decreases, the electron in charge resonant states is not stable, and will release because it is far from the ionized atom and misses the peak laser field. The electrons can achieve less drift momenta from the laser field, resulting in narrower longitudinal momentum distributions. Second, the recaptured electrons in the charge oscillation states will significantly blur above-threshold ionization peaks [23] (for details see [24]). As seen in Fig. 2, above-threshold ionization peaks of dimers are not prominent as compared with those of atoms. Third, the electrons in the charge resonant states coupled by strong laser fields will counteract the dimer dissociation through the channel of  $RG_2^+ \rightarrow RG^+ + RG$  when the internuclear distance of the dimer ions shrinks to

the equilibrium position (e.g., 2.48 Å for  $Ar_2^+$  and 2.77 Å for  $Kr_2^+$ ). For the hard bonding molecules, it is more reasonable to expect a larger probability of molecular dissociation at such larger internuclear distance. Indeed, there are a large amount of stable dimer ions  $RG_2^+$  (>90%) remaining in the laser fields for single ionization of dimers. This indicates a form of molecular stabilization at large internuclear distance, akin to the dressed state of molecular stabilization to suppress the dissociation [25].

One should note that, for tunneling ionization of  $Kr_2$  at 1320 nm, the photoelectron momentum distribution is slightly narrower than that of Kr. The observation suggests that the spin-orbit coupling effect [14] may have an important effect on strong-field ionization of Kr dimers because it will induce a larger energy splitting of those ionic states. Besides that, the larger internuclear distance of  $Kr_2$  compared to  $Ar_2$  may also play a role. Both those effects will increase the charge oscillation period for  $Kr_2$ .

In summary, we have investigated the wavelength, intensity, and ellipticity dependence of strong-field ionization of the RG dimers, i.e.,  $Ar_2$  and  $Kr_2$ . In the multiphoton ionization regime, the longitudinal drift momentum distributions of the RG dimers are much narrower than that of the RG atoms at the same laser intensity. Instead, in the tunneling regime, the photoelectron longitudinal momentum distributions of the dimers and the monomers show similar momentum distributions at the same laser intensity. We verify that tunneling ionization of dimers is mainly through the ionization of one of nearly independent “atoms.” The charge oscillation facilitated by electron recollision dominates multiphoton ionization of the dimers. Our qualitative explanation sheds light on strong-field ionization of molecules with larger internuclear distance. Our findings bring both challenges and opportunities for quantitative models for strong-field ionization of dimers.

We acknowledge the support of the 973 program (Grant No. 2013CB922403), the NSFC (Grants No. 11121091 and No. 11134001). Y.L. acknowledges the support by NSFC for Distinguished Young Scholars (Grant No. 11125416).

- 
- [1] L. S. Cederbaum, J. Zobeley, and F. Tarantelli, *Phys. Rev. Lett.* **79**, 4778 (1997).
- [2] J. Zobeley, R. Santra, and L. S. Cederbaum, *J. Chem. Phys.* **115**, 5076 (2001).
- [3] Z. Ansari, M. Böttcher, B. Manschwetus, H. Rottke, W. Sandner, A. Verhoef, M. Lezius, G. G. Paulus, A. Saenz, and D. B. Milošević, *New J. Phys.* **10**, 093027 (2008); A. vonVeltheim, B. Manschwetus, W. Quan, B. Borchers, G. Steinmeyer, H. Rottke, and W. Sandner, *Phys. Rev. Lett.* **110**, 023001 (2013).
- [4] B. Manschwetus, H. Rottke, G. Steinmeyer, L. Foucar, A. Czasch, H. Schmidt-Böcking, and W. Sandner, *Phys. Rev. A* **82**, 013413 (2010).
- [5] B. Ulrich, A. Vredenborg, A. Malakzadeh, M. Meckel, K. Cole, M. Smolarski, Z. Chang, T. Jahnke, and R. Dörner, *Phys. Rev. A* **82**, 013412 (2010).
- [6] J. Wu, A. Vredenborg, B. Ulrich, L. Ph. H. Schmidt, M. Meckel, S. Voss, H. Sann, H. Kim, T. Jahnke, and R. Dörner, *Phys. Rev. Lett.* **107**, 043003 (2011).
- [7] L. V. Keldysh, *Zh. Eksp. Teor. Fiz.* **47**, 1945 (1964) [*Sov. Phys. JETP* **20**, 1307 (1965)].
- [8] Y. Liu, X. Liu, Y. Deng, C. Wu, H. Jiang, and Q. Gong, *Phys. Rev. Lett.* **106**, 073004 (2011).
- [9] Y. Deng, Y. Liu, X. Liu, H. Liu, Y. Yang, C. Wu, and Q. Gong, *Phys. Rev. A* **84**, 065405 (2011).
- [10] J. Ullrich, R. Moshhammer, A. Dorn, R. Dörner, L. Ph. H. Schmidt, and H. Schmidt-Böcking, *Rep. Prog. Phys.* **66**, 1463 (2003).
- [11] F. H. M. Faisal, *J. Phys. B* **6**, L89 (1973).
- [12] H. R. Reiss, *Phys. Rev. A* **22**, 1786 (1980).
- [13] P. M. Dehmer, *J. Chem. Phys.* **76**, 1263 (1982); P. M. Dehmer and J. L. Dehmer, *ibid.* **69**, 125 (1978).
- [14] C. Y. Ng, D. J. Trevor, B. H. Mahan, and Y. T. Lee, *J. Chem. Phys.* **66**, 446 (1977).
- [15] M. Li, Y. Liu, H. Liu, Q. Ning, L. Fu, J. Liu, Y. Deng, C. Wu, L. Peng, and Q. Gong, *Phys. Rev. Lett.* **111**, 023006 (2013) [for the structure of the longitudinal momentum distribution of He

- and Ne, see A. Rudenko, K. Zrost, C. D. Schröter, V. L. B. de Jesus, B. Feuerstein, R. Moshhammer, and J. Ullrich, *J. Phys. B* **37**, L407 (2004)].
- [16] M. V. Ammosov, N. B. Delone and V. P. Krainov, *Zh. Eksp. Teor. Fiz.* **91**, 2008 (1986) [*Sov. Phys. JETP Lett.* **64**, 1191 (1986)]; N. B. Delone and V. P. Krainov, *J. Opt. Soc. Am. B* **8**, 1207 (1991).
- [17] K. J. Schafer, B. Yang, L. F. DiMauro, and K. C. Kulander, *Phys. Rev. Lett.* **70**, 1599 (1993); P. B. Corkum, *ibid.* **71**, 1994 (1993).
- [18] T. Nubbemeyer, K. Gorling, A. Saenz, U. Eichmann, and W. Sandner, *Phys. Rev. Lett.* **101**, 233001 (2008).
- [19] U. Eichmann, T. Nubbemeyer, H. Rottke, and W. Sandner, *Nature* **461**, 1261 (2009).
- [20] H. Liu, Y. Liu, L. Fu, G. Xin, D. Ye, J. Liu, X. T. He, Y. Yang, X. Liu, Y. Deng, C. Wu, and Q. Gong, *Phys. Rev. Lett.* **109**, 093001 (2012).
- [21] W. R. Wadt, *J. Chem. Phys.* **68**, 402 (1978).
- [22] T. Zuo and A. D. Bandrauk, *Phys. Rev. A* **52**, R2511 (1995).
- [23] P. Agostini, F. Fabre, G. Mainfray, G. Petite, and N. K. Rahman, *Phys. Rev. Lett.* **42**, 1127 (1979).
- [24] M. Li, Y. Liu, H. Liu, Y. Yang, J. Yuan, X. Liu, Y. Deng, C. Wu, and Q. Gong, *Phys. Rev. A* **85**, 013414 (2012).
- [25] E. E. Aubanel, J.-M. Gauthier, and A. D. Bandrauk, *Phys. Rev. A* **48**, 2145 (1993); E. E. Aubanel, A. Conjusteau, and A. D. Bandrauk, *ibid.* **48**, R4011 (1993).